Available online at www.sciencedirect.com
SCIENCE DIRECT
Catalysis Today 102–103 (2005) 67–77
CATALYSIS TODAY
www.elsevier.com/locate/cattod

Oxidation of limonene over carbon anchored transition metal Schiff base complexes: Effect of the linking agent

P. Oliveira [a], A.M. Ramos [a], I. Fonseca [a], A. Botelho do Rego [b], J. Vital [a,*]

[a] *REQUIMTE-Departamento de Química, CQFB, FCT-UNL, 2829-516 Caparica, Portugal*
[b] *CQFM-CI, IST, Av. Rovisco Pais, 1049-001 Lisboa, Portugal*

Available online 24 March 2005

Abstract

The oxidation of limonene over carbon anchored cobalt acetylacetonate catalysts is reported. The reaction is carried out in batch reactor, at 60 °C, in the solvent system acetone:*t*-butanol, with *t*-butyl hydroperoxide as oxygen supplier. Complex anchoring was achieved in four consecutive steps: (i) oxidation of activated carbon with nitric acid, (ii) treatment with thionyl chloride that converts the free carboxylic acid surface groups into acyl chloride functionalities, (iii) reaction between the carbon surface acyl chloride functionalities and linear diamines used as linking agents and (iv) Schiff condensation between the remaining free amino group of the linking agent and the acetylacetonate complex. The resulting carbon-based materials were characterised by X-ray photoelectron spectroscopy (XPS), DRIFT, nitrogen adsorption isotherms and temperature-programmed desorption. Ethylenediamine, tetramethylenediamine, hexamethylenediamine and dodecamethylenediamine are used as linking agents. Two different carbon supports are prepared by oxidising the parent activated carbon with 1 M HNO_3 or 13 M HNO_3 in order to obtain support surfaces with different oxygen contents. The effects of the chain length of the linking agent as well as the support's oxygen content on the orientation of the reaction towards epoxidation or autoxidation is discussed.

Keywords: Limonene oxidation; Activated carbon; Anchored complexes; Schiff base cobalt(II) complexes

1. Introduction

Limonene is the main component of citrus oil being easily obtained from the fruit peel waste. It is usually epoxidised via the stoichiometric peracid route; however, this process is becoming unacceptable due to environmental reasons. Limonene epoxide is a key raw material for a wide variety of products, such as pharmaceuticals, perfumes and food additives. Limonene epoxidation may be obtained either by allylic oxidation or by epoxidation reaction. Allylic oxidation takes place usually via a free radical chain reaction pathway; it generally occurs when the intermediate metallic species are in a low oxidation state [1]. On the other hand, epoxide formation is more likely to occur when oxometallic species, like $O{=}Mn^{V}$, $O{=}Ru^{VIII}$, among others, are present [2]. However, both mechanisms may occur simultaneously, since other variables than the nature of the metallic species (e.g. the stability of the radicals formed), must be taken into account.

Cobalt salts have proved to be effective catalysts on limonene oxidation, leading to interesting products such as carveols and carvone [3,4]. It was established that the catalyst activity regarding the oxidation of unsaturated hydrocarbons is based on Co(III), which is formed during oxidation. However, other studies have proposed that Co(III) interacts with the double bond, forming a very reactive radical cation [4]. Transition metal complexes have been extensively used in homogeneous catalysis; however, separation of the catalysts is usually troublesome. To overcome this limitation, metal complexes have been immobilised in several supports. Numerous attempts have been made to immobilise homogeneous Schiff base complexes, such as, anchoring these complexes on a polymeric matrix [5]. Encapsulation [6–8], entrapment [9] and anchoring of metal bases onto porous inorganic supports [10,11] have also been reported.

Activated carbons can satisfy most of the desirable requirements for a suitable support: high surface area and good porosity, chemical inertness, stability, mechanical resistance. Activated carbons with different characteristics

* Corresponding author. Tel.: +351 212948385; fax: +351 212948385.
E-mail address: jmv@dq.fct.unl.pt (J. Vital).

0920-5861/$ – see front matter © 2005 Elsevier B.V. All rights reserved.
doi:10.1016/j.cattod.2005.02.034

can be prepared either by thermal or chemical processes, in order to achieve the desired catalytic performance [12]. The nature and type of the carbon surface groups influence the catalytic activity. As previously reported [13,14] the hydrophilic/hydrophobic balance of the activated carbons can influence the catalytic activity of the immobilised metal complexes. The oxygen containing groups present on carbon surface allow a wide range of strategies to covalently attach cobalt acetylacetonate complexes [15,16]. Anchoring the complexes is a way of preventing the catalyst leaching. The successful preparation of cobalt acetylacetonate anchored on activated carbon and its use in pinane oxidation to pinane hydroperoxide, was also reported in a previous work [15].

This work reports the oxidation of limonene in the liquid phase, over cobalt acetylacetonate Schiff base complexes, anchored on activated carbon, using *tert*-butyl hydroperoxide (*t*-BHP) as oxygen donor. The catalysts were prepared by using an amidisation technique previously reported [15,17] in which several diamines, with different chain length, were used as binding agents. The effects of the chain length of diamines, as well as the effect of the support's oxygen content, are discussed.

2. Experimental

2.1. Materials and solvents

A commercially available activated carbon (NORIT GAC 1240 PLUS) was used as the starting carbon material (Cin). The reagents used in the modification of Cin as well as in the anchoring of the Schiff base complex, were used as received. The solvents used were dehydrated with pre-activated molecular sieves, before use. The cobalt acetylacetonate complex ($Co(II)(acac)_2$), 1,2-diaminoethane, tetramethylenediamine, hexamethylenediamine, dodecamethylenediamine, *t*-butyl-hydroperoxide (70 wt.%), were purchased from Aldrich. Tionyl chloride, chloroform, acetone, ethanol and toluene were purchased from Merck. Limonene (98%) was supplied by Fluka.

2.2. Catalyst preparation

2.2.1. Oxidation of the activated carbon

Two types of activated carbon supports with different oxidation levels were prepared by refluxing Cin (as supplied carbon sample) with a 13 M nitric acid solution, for 6 h (support C^{13M}), or with a 1 M nitric acid solution, for 3 h (support C^{1M}). In both cases, a ratio of 1 g carbon:18 ml acid solution was used. The oxidised carbon materials obtained were separated by filtration, washed with distilled water until pH $\sim$ 7 and dried overnight at 90 °C.

2.2.2. Anchoring of linking agents

Supports C^{13M} and C^{1M} were refluxed with thionyl chloride (0.1 mol $SOCl_2$ per g carbon) for 1 h. The remaining $SOCl_2$ was distilled off. The so obtained carbon materials were designated as sample C^{13M}(TC) and C^{1M}(TC). The carbons functionalised with acyl chloride groups were refluxed with a 0.05 M toluene solution of a diamine, for 6 h. The solid material was extensively washed with ethanol and dried at 90 °C overnight.

2.2.3. Reaction with Co(II)(acac)$_2$

The activated carbon functionalised with the different diamines were refluxed with a 7×10^{-5} M chloroform solution of $Co(II)(acac)_2$, for 16 h. Finally, the so obtained catalysts were washed with ethanol and dried at 90 °C overnight (Table 1).

2.2.4. Adsorption of Co(II)(acac)$_2$

The support sample C^{13M} was refluxed with a 7×10^{-5} M chloroform solution of $Co(II)(acac)_2$, for 16 h. After this treatment the material was washed with ethanol and dried overnight at 90 °C. The so obtained material was designated $Co(acac)_2@C^{13M}$ (Table 1).

2.3. Catalyst characterisation

The textural characterisation of the carbon-based materials was obtained from physical adsorption of nitrogen at 77 K on a Micrometrics ASAP 2010 V1.01 B instrument. The surface area was calculated using the BET equation. The micropore volume and the mesopore surface area were determined by applying the so-called *t*-method, using the standard isotherm for carbon materials proposed by Reinoso et al. [18]. The total pore volume was estimated to be the liquid volume of nitrogen at a relative pressure of about 0.95 ($V_{0.95}$). The external volume was obtained by subtracting the micropore volume to the total pore volume [19]. The point of zero charge (PZC) was determined by mass titration [20,21].

Inductively coupled plasma (ICP) atomic emission spectroscopy was performed in a Jobin-Yvon (Ultima) instrument.

Elemental analyses of C, H, N and S were performed in an Automatic CHNS-O Elemental Analyser Flash EATM.

The carbon supports were characterised by temperature-programmed desorption/mass spectrometry (TPD–MS) analysis on a MICROMERITICS TPD/TPR 2900 instrument. TPD analyses were carried out by heating the samples

Table 1
List of the catalysts prepared

Catalysts	Linking agent
$Co(acac)_2@C^{13M}$	–
$[Co(acac)_2etd]@C^{13M}$(TC)	$NH_2(CH_2)_2NH_2$
$[Co(acac)_2tmd]@C^{13M}$(TC)	$NH_2(CH_2)_4NH_2$
$[Co(acac)_2hxd]@C^{13M}$(TC)	$NH_2(CH_2)_6NH_2$
$[Co(acac)_2dcd]@C^{13M}$(TC)	$NH_2(CH_2)_{12}NH_2$
$[Co(acac)_2etd]@C^{1M}$(TC)	$NH_2(CH_2)_2NH_2$
$[Co(acac)_2tmd]@C^{1M}$(TC)	$NH_2(CH_2)_4NH_2$
$[Co(acac)_2hxd]@C^{1M}$(TC	$NH_2(CH_2)_6NH_2$
$[Co(acac)_2dcd]@C^{1M}$(TC)	$NH_2(CH_2)_{12}NH_2$

in a U-shaped quartz tubular micro-reactor, in flowing He (25 cm^3/min, 0.1 MPa) with a heating rate of 10 °C/min until 950 °C. The evolution of CO (*m/z*, 28) and CO_2 (*m/z*, 44) was monitored with a FISONS MD800 GCMS instrument.

X-ray photoelectron spectroscopy (XPS) analysis was carried out on a XSAM800 (KRATOS, Manchester, UK) X-ray spectrometer operated in the fixed analyser transmission (FAT) mode with a pass energy of 20 eV, being used a non-monochromatic radiation from Mg anode (main $h\nu = 1253.6$ eV). Pressure in the analysis chamber: in the range of 1×10^{-9} Torr; power: 130 W.

FTIR spectroscopy of the powdered samples was carried out on a BIO-RAD FTS 155 spectrometer, by using a diffuse reflectance cell. The spectra were taken with a resolution of 4 cm^{-1}, by running 1500 scans.

2.4. Catalytic experiments

The reactions were carried out in a batch reactor at 60 °C, under atmospheric pressure and magnetic stirring, using an excess of oxidant, i.e. *t*-butyl hydroperoxide 70% (w/w) aqueous solution and a mixture of acetone and *t*-butanol as solvent (9:1 molar ratio). Typically, the reactor was loaded with 0.0145 mol of limonene and the oxygen donor, in a 1:8 molar ratio along with 50 mg of catalyst and 50 ml of solvent. For the catalyst [$Co(acac)_2$etd]@C^{1M}(TC) it was also carried out an experiment using a 1:2 molar ratio limonene/*t*-BHP, being kept all the other reaction conditions. Samples were taken periodically and analysed by GC and GC–MS on a 30 m × 0.25 mm DB-1 column from J&W, being used *n*-nonane as internal standard. Stability tests were performed for the catalyst sample [$Co(acac)_2$hxd]@C^{1M}(TC), by running three consecutive experiments. After each experiment the catalyst was recovered by filtration, thoroughly washed and used in the next experiment. A hot-filtration test [22] was carried out for the catalyst sample [$Co(acac)_2$etd]@C^{1M}(TC). The reaction was carried out as described above; after 4 h (limonene conversion 41%) the catalyst was removed by hot-filtration. Sampling of the liquid phase was continued until 52 h after the experiment have been started.

3. Results and discussion

3.1. Catalyst preparation

The immobilisation of the cobalt acetylacetonate on the surface of the activated carbon support followed the methodology previously reported [15]: (a) oxidation of the activated carbon samples with nitric acid solutions of different concentrations, in order to generate acid carboxylic groups onto the surface; (b) reaction with $SOCl_2$ in order to convert the acid carboxylic groups into acyl chloride groups; (c) esterification of those acyl chloride groups with diamines of different chain. Finally, (d) anchoring of the cobalt acetylacetonate complex on the free amino groups via Schiff coupling reaction (Scheme 1).

3.2. Catalyst characterisation

3.2.1. Temperature-programmed desorption

The oxidised carbon supports C^{13M} and C^{1M} were characterised by TPD–MS, monitoring the CO and the CO_2 released upon heating of the samples. The TPD–MS spectra are composite of CO and CO_2 peaks. The surface composition can be estimated by deconvoluting those peaks

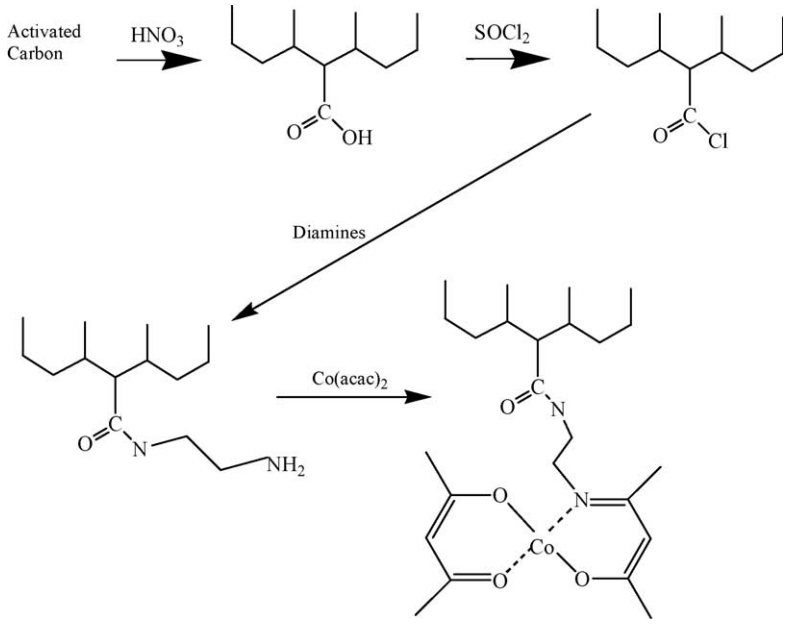

Scheme 1.

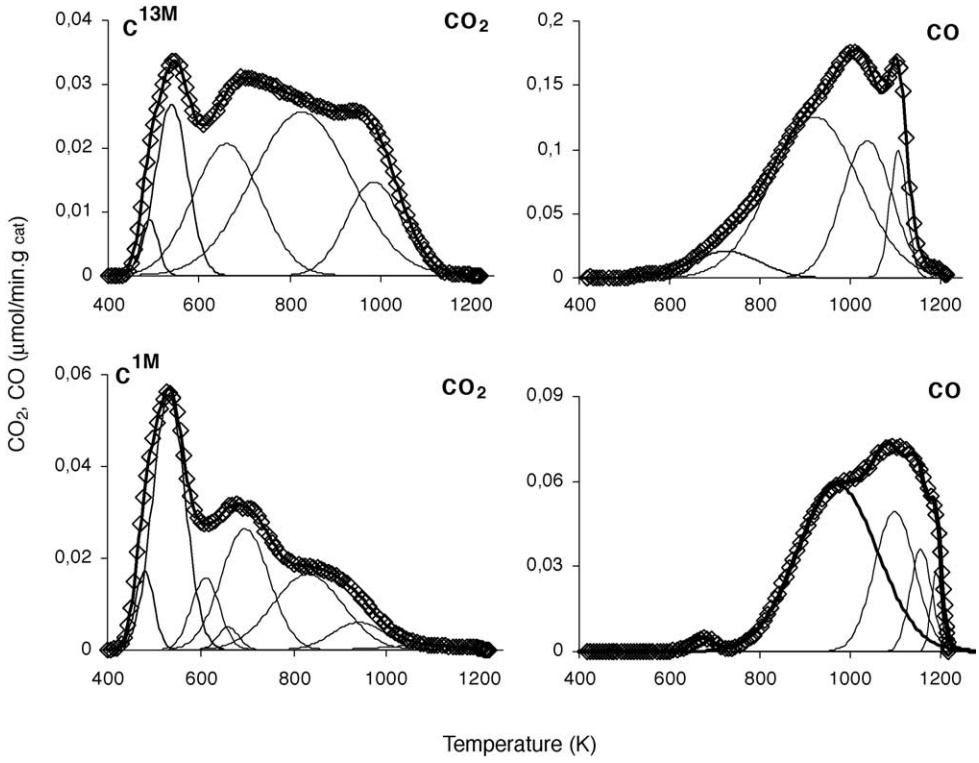

Fig. 1. CO and CO_2 TPD profiles of samples C^{13M} and C^{1M} and deconvolution curves.

[23,24]. The amount of the surface functional groups yielding CO_2 and/or CO within a given temperature range can be calculated by integrating the corresponding deconvolution bands. There is some controversy in literature concerning to the assignment of the TPD peaks to specific groups; however, some general trends have been established. Thus, CO_2 peaks results from carboxylic acids at low temperatures or from lactones at higher temperatures [23,24]; carboxylic anhydrides originate both CO and CO_2 peaks; phenols, ethers, carbonyls and quinones originate only the CO desorption profile.

The CO_2 and CO desorption profiles of samples C^{13M} and C^{1M} are depicted in Fig. 1. The peaks were assigned according to Table 2.

Fig. 2 shows the amount of surface groups calculated by integrating the TPD deconvolution bands. The support sample C^{13M} is the most oxidised one, being its surface composition dominated by phenol groups. Although carboxylic anhydrides and lactones are also present in higher amount in C^{13M} than in C^{1M}, the content of free carboxylic groups is lower in sample C^{13M} than in sample C^{1M}. The PZC values of 5.2 and 3.42, observed, respectively, for samples C^{13M} and C^{1M}, correlate quite well with these results. The higher content in free carboxylic groups of the less oxidised carbon sample, C^{1M}, may be explained by the softer oxidation conditions used (HNO_3, 1 M). In fact, being the carbon oxidation more extensive in sample C^{13M}, the number of phenol and total carboxylic groups generated on the surface is higher. Therefore, the probability of those groups lying closer each other is also higher than in sample C^{1M}, what explains the lower content of free carboxylic acids but the higher content of lactones and anhydrides, observed for the carbon sample C^{13M}.

3.2.2. CHNS elemental analysis

The CHNS elemental analysis of the carbon materials is shown on Table 3. Samples C^{13M} and C^{1M} exhibit smaller amounts of elemental carbon than the parent material Cin, as a consequence of the acid treatment. For all the anchored catalysts is observed an increase in the nitrogen content, reflecting the presence of the linking agents on the carbon materials.

3.2.3. Textural characterisation

All nitrogen adsorption–desorption isotherms of the carbon samples are type I as defined by IUPAC, characteristic of microporous carbons, with a small type

Table 2
Temperature ranges for the decomposition of the carbon surface functional groups

Surface group	Desorpted gas	Desorption temperature (K)	References
Carboxylic groups	CO_2	400–600	[26–29]
Carboxylic anhydrides	CO, CO_2	680–720	[25–29]
Lactones	CO_2	770–1100	[26]
Phenols	CO	980–1070	[26,27,30]
Carbonyl, quinones and ethers	CO	1073–1200	[26,30]

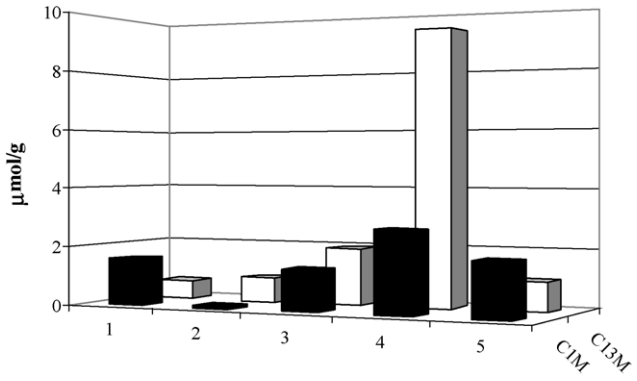

Fig. 2. Amounts of oxygen surface groups determined by integrating the TPD deconvolution curves for samples C^{13M} and C^{1M}: (1) free carboxylic acids; (2) carboxylic anhydrides; (3) lactones; (4) phenols; (5) hemiquinones, quinones, ethers.

H4 hysteresis loop. Table 4 shows the values of BET specific apparent surface area (S_{BET}), volume of micropores (V_{micro}), external surface area (S_{ext}), total pore volume calculated at $P/P_0 = 0.95$($V_{0.95}$), as well as the external volume (volume of macro + mesopores − V_{ext}), calculated as the difference between $V_{0.95}$ and V_{micro}. There are not significant textural differences between the original carbon, Cin, and the oxidised supports C^{1M} and C^{13M}, in agreement to what has being observed by other authors [21]. However, marked decreases in the total surface area, the micropore volume and external area are observed when the cobalt acetylacetonate is anchored onto the modified activated carbons (Table 4). These decreases are strong indications of the presence of voluminous molecules in the pore system of the carbon supports. Samples [$Co(acac)_2$dcd]@C^{13M}(TC) and [$Co(acac)_2$hxd]@C^{1M}(TC) showed the highest decreases in the micropore volume.

3.2.4. X-ray photoelectron spectroscopy

The ratio between the cobalt content, determined by XPS, and the total cobalt content, determined by ICP, yields information about the homogeneity of the distribution of the metal complex [28]. For all the catalyst samples, except for [$Co(acac)_2$]@C^{13M}, $\%M_{XPS}/\%M_{ICP}$ (Table 5) is much higher than unity. This is an indication that the cobalt acetylacetonate complex is heterogeneously distributed, being preferentially located on the external surface of the support particles. In these circumstances the voluminous complex molecules may be blocking the porous system of the carbon support justifying, therefore, the strong decrease observed in the micropore volume in relation to the parent material (Table 4). For sample [$Co(acac)_2$]@C^{13M}, that ratio is close to unity, which means that the metal complex is more homogeneously distributed on the support. Consequently, the molecules of the complex penetrate more deeply the porous system of the carbon particles. This conclusion is also supported by the observed fact that a decrease in the micropore volume similar to that observed for all the other catalyst samples is only achieved with higher complex loadings.

The lower O/C ratio exhibited by support C^{13M} in relation to support C^{1M} (Table 6), in apparent contradiction to the results obtained by TPD/MS, probably means that, in the case of sample C^{13M}, the oxygenated functional groups are

Table 3
Elemental analysis of the carbon-based materials

Sample	C%	N%	H%	S%
Cin	85.24	0.39	0.34	0.72
C^{13M}	73.93	0.61	0.49	0.44
$Co(acac)_2$@C^{13M}	75.22	0.71	1.26	–
[$Co(acac)_2$etd]@C^{13M}(TC)	71.21	3.00	1.36	0.69
[$Co(acac)_2$tmd]@C^{13M}(TC)	75.57	1.67	1.06	0.61
[$Co(acac)_2$hxd]@C^{13M}(TC)	74.27	2.49	1.43	0.52
[$Co(acac)_2$dcd]@C^{13M}(TC)	78.95	2.61	2.02	0.52
C^{1M}	71.44	0.63	0.42	0.45
[$Co(acac)_2$etd]@C^{1M}(TC)	69.33	3.46	1.36	0.87
[$Co(acac)_2$tmd]@C^{1M}(TC)	70.82	2.37	1.02	0.88
[$Co(acac)_2$hxd]@C^{1M}(TC)	72.26	2.43	1.28	0.74
[$Co(acac)_2$dcd]@C^{1M}(TC)	78.97	0.90	1.02	0.82

Table 4
Textural properties of the carbon-based materials

Sample	S_{BET}[a] (m^2/g)	V_{micro}[b] (cm^3/g)	S_{ext}[b] (m^2/g)	$V_{0.95}$[c] (cm^3/g)	V_{ext}[d] (cm^3/g)
Cin	777.0	0.39	94.20	0.54	0.14
C^{13M}	837.4	0.41	103.80	0.56	0.15
$Co(acac)_2$@ C^{13M}	693.6	0.34	86.13	0.47	0.13
[$Co(acac)_2$etd]@C^{13M}(TC)	519.2	0.26	82.97	0.34	0.08
[$Co(acac)_2$tmd]@C^{13M}(TC)	624.6	0.30	83.34	0.42	0.13
[$Co(acac)_2$hxd]@C^{13M}(TC)	429.2	0.18	76.03	0.30	0.12
[$Co(acac)_2$dcd]@C^{13M}(TC)	103.6	0.03	50.47	0.11	0.08
C^{1M}	893.0	0.43	95.37	0.57	0.15
[$Co(acac)_2$etd]@C^{1M}(TC)	581.2	0.26	87.89	0.39	0.13
[$Co(acac)_2$tmd]@C^{1M}(TC)	434.1	0.19	79.70	0.31	0.12
[$Co(acac)_2$hxd]@C^{1M}(TC)	206.8	0.07	70.57	0.18	0.11
[$Co(acac)_2$dcd]@C^{1M}(TC)	564.1	0.26	78.79	0.33	0.08

[a] BET surface area.
[b] Calculated by *t*-method.
[c] Total pore volume estimated at P/P_0 about 0.95.
[d] Calculated by subtracting V_{micro} from $V_{0.95}$.

Table 5
Metal content as determined by XPS and ICP analysis

Sample	$\%M_{XPS}$	$\%M_{ICP}$	$\%M_{XPS}/\%M_{ICP}$
$Co(acac)_2@C^{13M}$	1.84	0.99	1.87
$[Co(acac)_2etd]@C^{13M}(TC)$	3.73	0.47	8.00
$[Co(acac)_2tmd]@C^{13M}(TC)$	2.68	0.66	4.06
$[Co(acac)_2hxd]@C^{13M}(TC)$	2.44	0.85	2.88
$[Co(acac)_2dcd]@C^{13M}(TC)$	4.11	0.77	5.31
$[Co(acac)_2etd]@C^{1M}(TC)$	2.78	0.66	4.20
$[Co(acac)_2tmd]@C^{1M}(TC)$	1.36	0.50	2.68
$[Co(acac)_2hxd]@C^{1M}(TC)$	2.52	0.19	13.57
$[Co(acac)_2dcd]@C^{1M}(TC)$	3.35	0.44	7.66

preferentially located inside the particle pore system than on the outer surface. The chlorine content for samples $C^{13M}(TC)$ and $C^{1M}(TC)$ increases after the treatment with thionyl chloride, in relation to samples C^{13M} and C^{1M}.

The nitrogen content of all the catalyst samples (except for $Co(acac)_2@C^{13M}$) increases in relation to that of the carbon support samples. Simultaneously, a decrease in the chlorine content is also observed. These observations are indications that the esterification reaction between the diamines used as linking agents and the acyl groups of the support surface, was successful.

The Cl 2p spectra of carbons $C^{13M}(TC)$ and $C^{1M}(TC)$ show fitting peaks at about 200.45 eV, which are characteristic of chlorine covalently attached to carbon atoms (Fig. 3). These peaks are still present in the spectra of the anchored catalysts (therefore, after esterification with the linking agents), indicating that the reaction of the acyl chloride groups with the diamines is not complete. However, a new band appears in these spectra, with a binding energy of 198.5 eV, which is likely to be due to chloride ions and is also an indication that the esterification reaction was successful.

The high-resolution spectra of the catalyst samples (all but $Co(acac)_2@C^{13M}$) in the N 1s region show an intense peak at 400 eV (shown in Fig. 4 as an example for samples $[Co(acac)_2hxd]@C^{1M}$ and $[Co(acac)_2dcd]@C^{1M}$), which can be attributed to different types of nitrogen groups present in the carbon surface, such as amides, imines and amines [29]. Amide groups are expected to be present on the carbon surface as a consequence of the reaction between the acyl chloride groups and diamines. On the other hand, imine groups are also expected, after the anchoring of the cobalt acetylacetonate. These carbon catalysts also exhibit a fitting peak at about 401.5 eV (not shown), that may be assigned to quaternised nitrogen [30], which is likely to be present on the carbon surface. The anchoring reaction of diamines yields hydrogen chloride as a side product, which on its turn, can protonate the free amino groups.

All samples show an intense peak in the C 1s region, at about 285 eV (Fig. 5), characteristic of the graphitic carbon [31], and four peaks at higher binding energies, due to carbon in higher oxidation states.

For all the carbon samples the O 1s signal lies between 528 and 540 eV (exemplified in Fig. 6). For the anchored catalysts, an increase of the relative intensity of the peak at about 531.5 eV is observed, when compared with the carbon supports (C^{13M} and C^{1M}). This observation may suggest the presence of oxygen atoms in a different chemical environment as a result of the complex anchoring process, namely the formation of amide groups [29].

3.2.5. FTIR studies

The changes introduced on the parent activated carbon were also followed by infrared spectroscopy using a diffuse reflectance cell (DRIFT). The DRIFT spectra were run for all the carbon samples.

For all the anchored catalysts, three bands were observed on the characteristic absorptions of the amide group. Amide I band, at about 1670 cm^{-1} results mainly from ν(C=O); amide II and amide III, at about 1550 and 1296 cm^{-1} [32,33], respectively, arise as well from ν(C–N) as from δ(N–H), since this modes are coupled to one another. A new band is also observed in the spectra of all catalyst samples, except for catalyst $Co(acac)_2@C^{13M}$, at about 1630–1660 cm^{-1}, which is usually assigned to the imine group (C=N) [34].

Table 6
Area under the XPS bands in O 1s, C 1s, N 1s, Cl 2p and Co 2p regions for the carbon materials

Sample	Atomic %					O/C	N/C	Cl/C	Co/C
	C	O	N	Cl	Co				
Cin	94.1	5.80	–	–	–	0.06	–	–	–
C^{13M}	86.5	12.2	0.25	0.52	–	0.14	0.003	0.006	–
$C^{13M}(TC)$	85.1	12.3	–	1.88	–	0.14	0.000	0.022	–
$Co(acac)_2@C^{13M}$	85.4	12.8	0.51	0.51	0.40	0.15	0.006	0.006	0.005
$[Co(acac)_2etd]@C^{13M}(TC)$	84.2	10.6	4.09	0.25	0.39	0.13	0.049	0.003	0.005
$[Co(acac)_2tmd]@C^{13M}(TC)$	83.7	12.0	2.73	0.60	0.59	0.14	0.033	0.007	0.007
$[Co(acac)_2hxd]@C^{13M}(TC)$	84.7	11.1	2.81	0.46	0.54	0.13	0.033	0.005	0.006
$[Co(acac)_2dcd]@C^{13M}(TC)$	84.0	11.0	3.11	0.54	0.92	0.13	0.037	0.006	0.011
C^{1M}	88.1	13.9	0.84	0.00	–	0.16	0.010	0.000	–
$C^{1M}(TC)$	81.3	15.0	0.94	0.89	–	0.18	0.012	0.011	–
$[Co(acac)_2etd]@C^{1M}(TC)$	84.8	10.5	3.38	0.35	0.61	0.12	0.040	0.004	0.007
$[Co(acac)_2tmd]@C^{1M}(TC)$	85.6	9.50	2.95	0.27	0.29	0.11	0.034	0.003	0.003
$[Co(acac)_2hxd]@C^{1M}(TC)$	86.0	9.50	3.30	0.33	0.55	0.11	0.038	0.004	0.006
$[Co(acac)_2dcd]@C^{1M}(TC)$	87.5	9.40	1.17	0.60	0.74	0.11	0.013	0.007	0.008

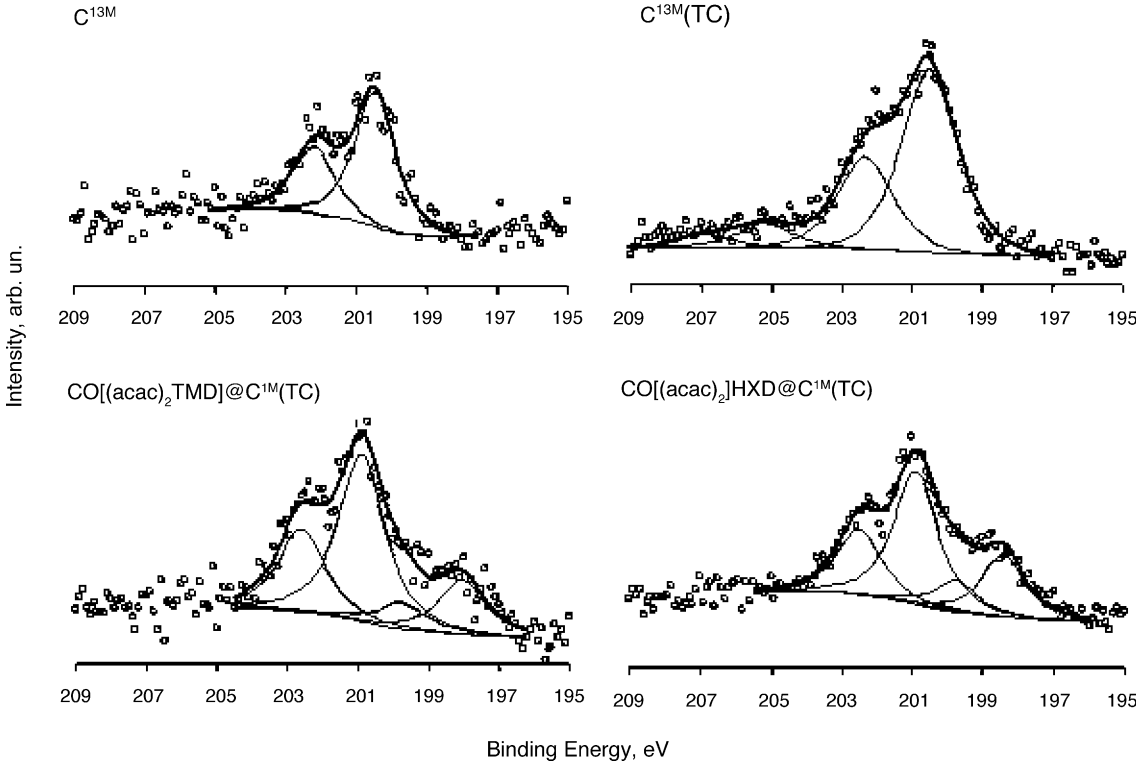

Fig. 3. High-resolution XPS spectra in the Cl 2p region.

As an example, Fig. 7, shows the spectra obtained for carbons C^{13M}, [$Co(acac)_2$etd@C^{13M}] and [$Co(acac)_2$]@C^{13M}. That new band at about 1630 cm^{-1} arises in the spectrum obtained for the catalyst sample [$Co(acac)_2$etd]@C^{13M}, while it is not present in the spectra of C^{13M} and [$Co(acac)_2$]@C^{13M}. This is an indication that the Schiff reaction between the terminal primary amines and the cobalt acetylacetonate complex was succeeded.

3.3. Catalytic experiments

For almost all the catalyst samples tested, the main product of the oxidation of limonene catalysed by the carbon anchored cobalt acetylacetonates, with *tert*-butyl hydroperoxide as oxygen supplier, in the solvent system acetone—*t*-butanol, is a polymer (analysis: C—65.55%; H—7.55%), being also formed minor amounts of carveol and carvone. A number of products such as perillyl alcohol, perillaldehyde, *p*-mentha-1(7),8-dien-2-ol, *p*-mentha-2,8-dien-1-ol, etc., as well as several unidentified GC peaks (all lumped on Table 7 and Fig. 10 as 'others') were also formed in trace amounts.

Table 8 shows the effect of the catalyst used on the polymer average molecular weight and polydispersity, for the catalyst samples [$Co(acac)_2$etd]@C^{13M}, [$Co(acac)_2$hxd]@C^{13M}, [$Co(acac)_2$dcd]@C^{13M}. For the experiment carried out with the catalyst sample [$Co(acac)_2$tmd]@C^{13M}(TC), however, no polymer is formed and the main products are carveol and carvone.

In order to investigate the origin of the obtained polymer, an experiment was carried out in which a small amount of

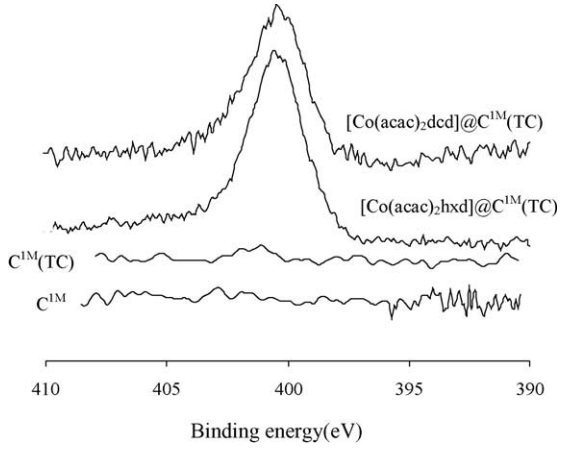

Fig. 4. High-resolution XPS spectra in the N 1s region.

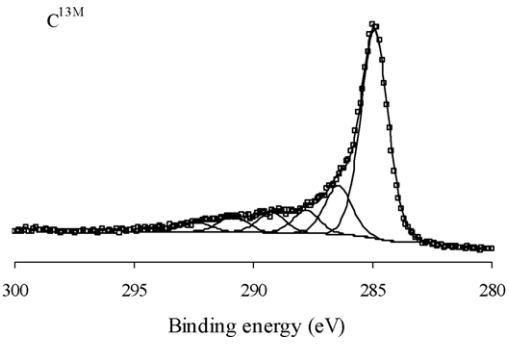

Fig. 5. High-resolution XPS spectrum in the C 1s region for support C^{13M}.

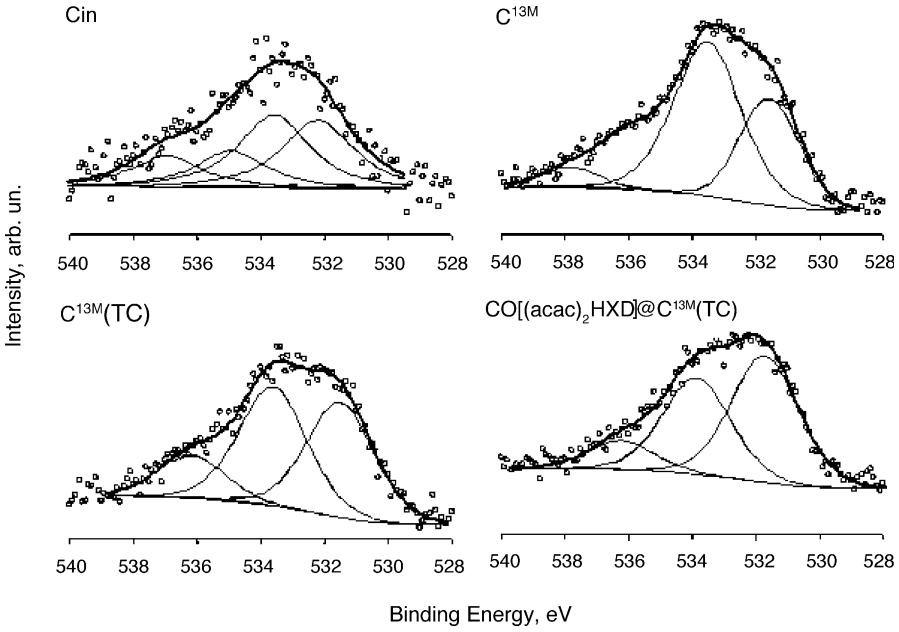

Fig. 6. High-resolution XPS spectra in the O 1s region.

limonene oxide was added to a sample of the reaction mixture, being observed immediate polymerisation. On the other hand, when the oxidation of limonene is carried out by using a much less concentrated *t*-BHP solution (3%, limonene/*t*-BHP molar ratio—1:2), a small amount of limonene oxide is detected. These results led us to the conclusion that the primary product of the oxidation of limonene is limonene oxide, which immediately polymerises under the reaction conditions used (homogeneous liquid phase, concentrated *t*-BHP).

The results of the catalytic experiments carried out with the anchored catalysts, are shown on Table 7 in terms of the initial turnover frequency (TOF), maximum limonene conversion and selectivity to the main products. Fig. 8 shows as examples, the concentration profiles and selectivity versus conversion plots for the catalyst samples [Co(acac)$_2$hxd]@C^{13M}(TC) and [Co(acac)$_2$etd]@C^{1M}(TC).

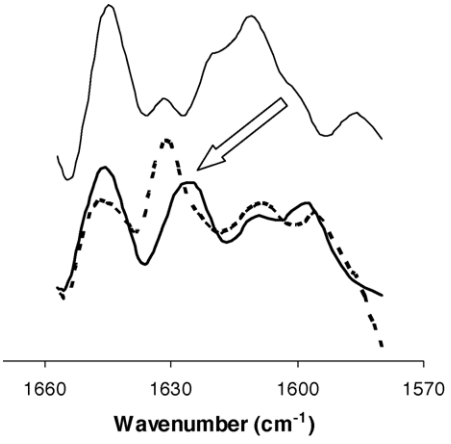

Fig. 7. FTIR spectra (absorvance scale) for samples: (—) C^{13M}, (—) [Co(acac)$_2$etd]@C^{13M}(TC) and (- - -) Co(acac)$_2$@C^{13M}.

In order to check the effect of the carbon support, two series of experiments were carried out: the C13M series, comprising the experiments performed with the most oxidised support (C^{13M}—Table 7, runs 1–5) and the C1M series, comprising the experiments performed with the less oxidised support (C^{1M}—Table 7, runs 6–9).

In a general way, higher initial TOFs are obtained in the C1M series than in the C13M series. On the other hand, initial TOF grows with the chain length of the linking agent (etd—C2, tmd—C4, hxd—C6 and dcd—C12), reaching a maximum value in both series, for the catalysts [Co(acac)$_2$hxd]@C^{13M}(TC) and [Co(acac)$_2$hxd]@C^{1M}(TC), which use hexamethylenediamine as linking agent. These observations may be explained on the basis of the hydrophilicity of the support surface. For the C13M series, the support exhibits the highest hydrophilic character. The reaction medium in the vicinity of the support's surface is likely to be poor in limonene and, therefore, TOF is low. For the C1M series, higher concentrations of limonene in the regions close to the carbon support are expectable, leading to the observed higher TOF values.

For both series, with the increase of the chain length of the linking agent, the complex is progressively collocated apart from the carbon surface (therefore, in regions that are richer in limonene). Consequently, higher initial TOF values are progressively observed. The exceptions, also observed for both series, are the catalysts linked with dodecamethylenediamine (dcd—C12). They may be explained by the bending of the long methylenic chain towards the support surface.

In what concerns selectivity, the main issue is the reaction orientation towards epoxidation or allylic oxidation, via a

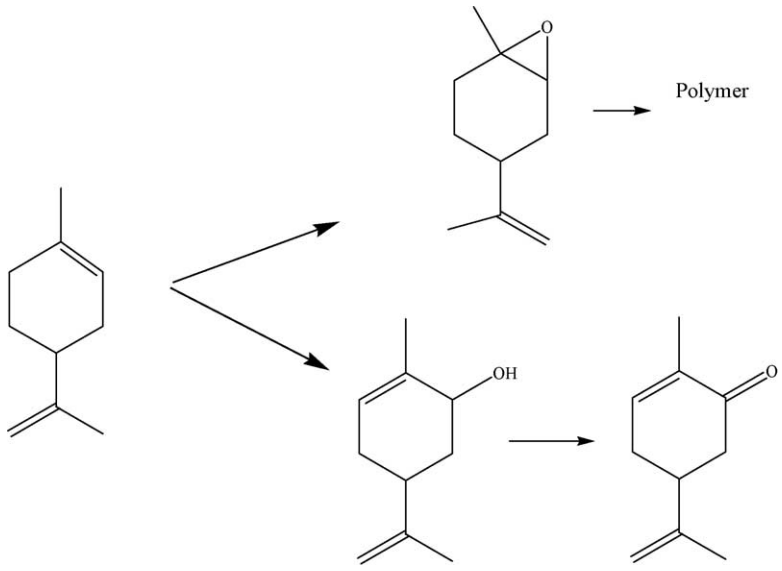

Scheme 2.

radical chain reaction mechanism [3] (Scheme 2). By comparing the results obtained with the catalysts bearing the same linking agent, selectivity to polymer (therefore, epoxide) is higher for series C1M than for series C13M, except for dcd (Table 7). This result suggests that epoxidation is the pathway preferred with the less hydrophilic support (C^{1M}).

According to literature, epoxidation only takes place if limonene molecules can reach the catalyst metal sites [35–38]. Therefore, the less hydrophilicity of support C^{1M} explains that reaction orientation, since the accessibility of limonene molecules to the metal sites is favoured.

The analysis of the effect of the chain length of the linking agents on selectivity is more difficult, since the results seem to be erratic. Other factors such as the heterogeneous distribution of the complex in the support particles or the possibility of metal coordination to the surface groups may have a strong influence.

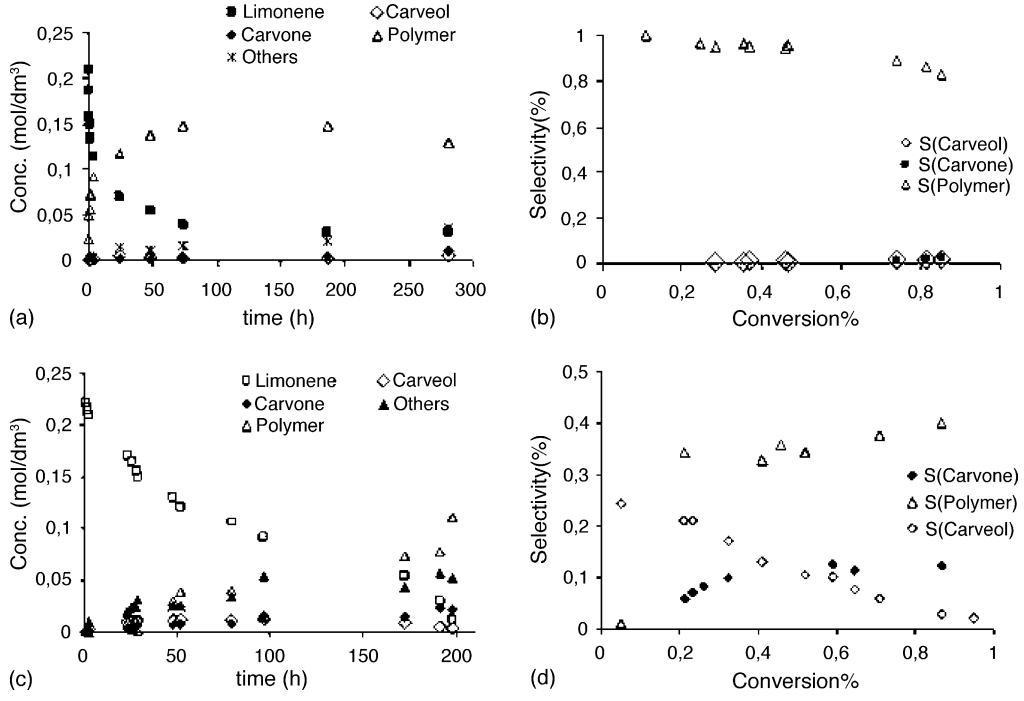

Fig. 8. Limonene concentration (a and c) and selectivity (b and d) profiles for the catalyst samples [$Co(acac)_2$etd]@C^{1M}(TC) and [$Co(acac)_2$hxd]@C^{13M}(TC), respectively.

Table 7
Limonene epoxidation catalysed by cobalt acetylacetonate anchored on activated carbon with different linking agents, using *t*-BHP as oxygen donor in a *t*-butanol/acetone solution

Run	Catalysts	Conversion[e] (%)	Product selectivity (%)[c]				TOF[d]
			Polymer	Carveol	Carvone	Others	
1	$Co(acac)_2@C^{13M}$	33.0[a]	7.1	6.7	6.6	79.0	15.60
2	$[Co(acac)_2etd]@C^{13M}$(TC)	95.0	21.1	7.8	11.3	59.0	8.9
3	$[Co(acac)_2tmd]@C^{13M}$(TC)	61.2	–	14.0	17.0	69.0	15.2
4	$[Co(acac)_2hxd]@C^{13M}$(TC)	93.1	67.6	5.0	5.1	22.0	36.6
5	$[Co(acac)_2dcd]@C^{13M}$(TC)	93.6[a]	92.0[b]	1.5[b]	2.9[b]	3.6[b]	31.3
6	$[Co(acac)_2etd]@C^{1M}$(TC)	85.5[a]	85.0[b]	2.3[b]	2.8[b]	9.9[b]	80.4
7	$[Co(acac)_2tmd]@C^{1M}$(TC)	88.6	53.8	6.7	6.5	33.0	165.3
8	$[Co(acac)_2hxd]@C^{1M}$(TC)	17.5[a]	80.0[b]	4.2[b]	7.9[b]	7.9[b]	441.2
9	$[Co(acac)_2dcd]@C^{1M}$(TC)	60.0	62.5	0.5	6.4	30.6	169.2

Conversion, selectivity and initial turnover frequency (TOF) for the catalytic experiments carried out over the catalyst samples.
[a] Maximum conversion obtained.
[b] Maximum selectivity obtained for the maximum conversion.
[c] Selectivity achieved for 60% of conversion.
[d] Turnover frequency.
[e] Conversion obtained when the reaction was stopped.

Table 8
Effect of the catalyst type on the polymer average molecular weight and polydispersity

Catalyst	$\bar{M}_w$	$\bar{M}_w/\bar{M}_n$
$[Co(acac)_2etd]@C^{13M}$(TC)	1160	1.8
$[Co(acac)_2hxd]@C^{13M}$(TC)	1363	1.7
$[Co(acac)_2dcd]@C^{13M}$(TC)	1188	1.6
$Co(acac)_2@C^{13M}$	857	1.7

Although the experiment carried out with the catalyst sample $[Co(acac)_2hxd]@C^{1M}$(TC) exhibits the highest initial TOF, the reaction seems to stop at a limonene conversion of only 17%, probably because all the *t*-butyl hydroperoxide was consumed. In fact, this catalyst sample exhibits the highest heterogeneity in the distribution of the metal complex (Table 4), being the cobalt Schiff complex massively located on the outer surface of the carbon particles. Therefore, the reactants have easy access to the metal centres. Limonene is readily oxidised, but also the hydroperoxide is easily decomposed by a redox mechanism [1]. In order to check the catalyst stability, three consecutive experiments were carried out with the same catalyst sample, which was recovered and re-used in the next experiment. The results, depicted in Fig. 9, show clearly that there is no loss in activity.

In order to confirm the catalyst stability, a hot-filtration experiment [22] was performed with the catalyst sample $[Co(acac)_2etd]@C^{1M}$(TC). After 4 h of reaction the catalyst was separated from the reaction mixture, and its composition was followed for more 48 h. Fig. 10 compares the limonene concentration profiles obtained for the hot-filtration experiment and a *normal* catalytic experiment, both performed with the same catalyst sample. It is quite clear that the reaction stops with the catalyst removing, while it continues proceeding in the *normal* experiment.

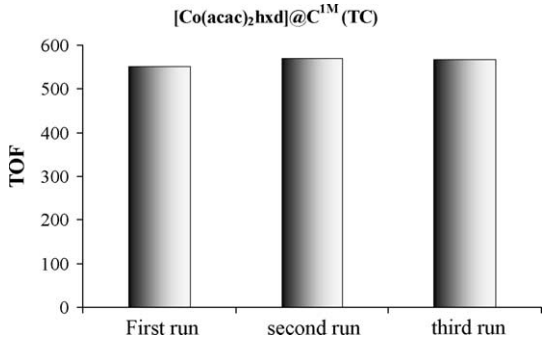

Fig. 9. Initial TOF obtained for three re-using experiments of the limonene oxidation catalysed by $[Co(acac)_2hxd]@C^{1M}$(TC).

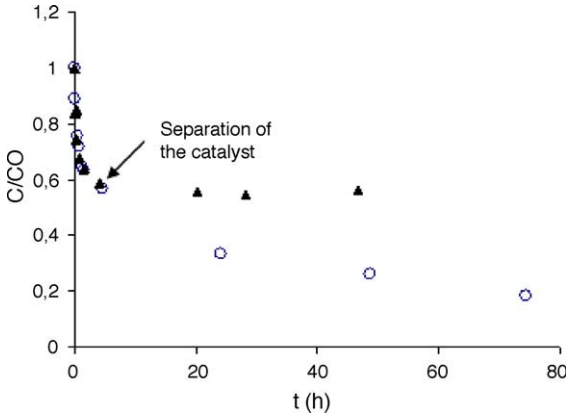

Fig. 10. Limonene concentration profiles obtained with the catalyst sample $[Co(acac)_2etd]@C^{1M}$(TC): (▲) hot-filtration test; (○) *normal* experiment.

4. Conclusions

The primary product of limonene oxidation over the carbon anchored cobalt acetylacetonates is likely to be limonene oxide, which however, polymerises instantly under the experimental conditions used.

The catalyst activity expressed as the initial turnover frequency seems to be strongly dependent both on the hydrophilic/hydrophobic balance of the carbon support and on the chain length of the linking agent. In a general way, initial TOF increases with the hydrophobicity of the carbon support and with the chain length of the linking agent. Generally, for the catalysts bearing the same linking agent, selectivity to limonene oxide/polymer is higher for the supports with lower oxygen content. However, its dependence on the linking agent chain length is not clear.

The anchored catalysts seem to be stable, since one of the catalyst samples keeps its activity in three consecutive re-using experiments, and other of the catalyst samples passed successfully a hot-filtration test.

The results obtained seem to be consisting with a two pathways mechanism, one corresponding to the epoxidation of the olefin on the metal centres, and the other corresponding to the limonene autoxidation via a free radical chain reaction.

Acknowledgements

The authors thank NORIT N.V., Amersfoort, The Netherlands, for providing the activated carbon. This work was carried out with support from the POCTI-FEDER Programme. P. Oliveira acknowledges the grant received under the same programme.

References

[1] R.A. Sheldon, J.K. Kochi, Metal-Catalysed Oxidations in Organic Compounds, Academic Press, New York, USA, 1981.
[2] R.A. Sheldon, J. Mol. Catal. 20 (1983) 1.
[3] M.J. Silva, P. Robles-Dutenhefner, L. Menini, E.V. Gusevskaya, J. Mol. Catal. 201 (2003) 71.
[4] M. Gomes, O.A.C. Antunes, J. Mol. Catal. 127 (1997) 145.
[5] Q.H. Fan, Y.M. Li, A.C. Chan, Chem. Rev. 102 (2002) 3385.
[6] C. Schuster, W.F. Hölderich, Catal. Today 60 (2000) 193.
[7] A. Valente, J. Vital, J. Mol. Catal. 156 (2000) 163.
[8] J. Pires, J. Francisco, A. Carvalho, M. Brotas de Carvalho, A. Silva, C. Freire, B. de Castro, M.M.A. Freitas, Langmuir 20 (2004) 2861.
[9] A. Corma, V. Fornes, F.R.A. Cervilla, E. Liopis, A. Ribera, J. Catal. 152 (1995) 237.
[10] A.R. Silva, C. Freire, B. De Castro, M.M.A. Freitas, J.L. Figuiredo, Micropor. Mesopor. Mater. 46 (2001) 211.
[11] C. Baleizão, B. Gigante, D. Das, M. Álvaro, H. Garcia, A. Corma, J. Catal. 223 (2004) 106.
[12] F. Rodrıguez-Reinoso, Activated carbon-structure, characterization, preparation and applications, in: H. Marsh, et al. (Eds.), Introduction to Carbon Technologies, University of Alicante, Secretariado de Publicaciones, Alicante, 1997, p. 35.
[13] F.T. Starzyk, M.V. Puymbroeck, R.F. Parton, P.A. Jacobs, J. Mol. Catal. 109 (1996) 75.
[14] A. Valente, C. Palma, M.J. Reis, I.F. Silva, A.M. Ramos, J. Vital, Carbon 41 (2003) 2793.
[15] A. Valente, A.M. Botelho do Rego, M.J. Reis, I.F. Silva, A.M. Ramos, J. Vital, Appl. Catal. A Gen. 207 (2001) 221.
[16] A.R. Silva, C. Freire, B. de Castro, M.M.A. Freitas, J.L. Figuiredo, Micropor. Mesopor. Mater. 46 (2001) 211.
[17] A.R. Silva, M. Martins, M.M.A. Freitas, J.L. Figueiredo, C. Freire, B. de Castro, Eur. J. Inorg. Chem. (2004) 2027.
[18] F.R. Reinoso, J.M.M. Martinez, C.P. Burguet, B. McEaney, J. Phys. Chem. 91 (1987) 515.
[19] Z. Hu, M.P. Srinivasan, Micropor. Mesopor. Mater. 43 (2001) 267.
[20] I. Such-Basánez, M.C. Román-Martínez, C. Salinas-Martínez de Lecea, Carbon 42 (2004) 1357.
[21] J.S. Noh, J.A. Schwarz, Carbon 28 (1990) 675.
[22] R.A. Sheldon, I.W.C.E. Arends, H.E.B. Lempers, Catal. Today 41 (1998) 387.
[23] S.G. Szymanski, Z. Karpinski, S. Biniak, A. Swiatkowski, Carbon 40 (2002) 2627.
[24] J.L. Figueirdo, M.F.R. Pereira, M.M.A. Freitas, J.J.M. Órfão, Carbon 37 (1999) 1379.
[25] C.M. Casttilla, F.C. Marín, F.M. Hódar, J.R. Utrilla, Carbon 36 (1998) 145.
[26] Y. Otake, R. Jenkins, Carbon 31 (1993) 109.
[27] Z. Hu, M.P. Srinivasan, Micropor. Mesopor. Mater. 43 (2001) 267.
[28] C.M. Casttilla, A.P. Cadenas, F.M. Hódar, F.C. Marín, J.L. Fierro, Carbon 41 (2003) 1157.
[29] R.J. Jansen, H. van Bekkum, Carbon 32 (1994) 1507.
[30] D.A. Buttry, J. Peng, J.B. Donnet, S. Rebouillat, Carbon 37 (1999) 1929.
[31] Z.R. Yue, W. Jiang, S.D. Gardner, C.U. Pittman Jr., Carbon 37 (1999) 1785.
[32] C. Jubert, A. Mohamadou, C. Gérard, S. Brandes, A. Tabard, BarbierF J.P., Inorg. Chem. Commun. 6 (2003) 900.
[33] M. Amirnars, K. Schenk, S. Meghdadi, Inorg. Chim. Acta 338 (2002) 19–26.
[34] K. Nakanishi, P.H. Solomon, Infrared Absorption Spectroscopy, Holden-Day Inc., London, 1977.
[35] J.D. Koola, J.K. Kochi, J. Org. Chem. 52 (1987) 4545.
[36] S. Wang, B. Mandimutsira, R. Todd, B. Ramdhanie, J. Fox, D. Goldberg, J. Am. Chem. Soc. 126 (2004) 18.
[37] W. Adam, K. Roschann, C. Möller, D. Seebach, J. Am. Chem. Soc. 124 (2002) 5068.
[38] L. Firdoussi, A. Baqqa, S. Allaoud, B. Allal, A. Karim, Y. Castanet, A. Mortreux, J. Mol. Catal. 135 (1998) 11.